Chemistry: Bulgarian Journal of Science Education *Volume 26 Number 4, 2017* *Природните науки в образованието*

KINETICS OF PHOTO-ELECTRO-ASSISTED DEGRADATION OF REMAZOL RED 5B

Fitria Rahmawati, Tri Martini, Nina Iswati
Sebelas Maret University – Indonesia

Abstract. This research studies a kinetics of photo-electro-assisted degradation of dyes. The kinetics study applied the Buttler-Volmer kinetics for electro-assisted reaction in combination with the regular chemical kinetics for photodegradation. The result then being compared with the regular chemical kinetics application for both photo-electro-assisted degradation. The degradation cell was designed by separating the anodic and cathodic cell, in which the dye solution was placed in the anodic cell. As the solvent, water molecules, also be able to undergo electro-oxidation, therefore in this research pH of the solution was recorded during reaction whether in the anodic or cathodic cell. The result shows that oxidation of H_2O occured in an anodic cell in competition with the dye oxidation. However, the dye oxidation proceeds faster than H_2O oxidation. In which, the rate constant of dye oxidation is 2.7795×10^{-3}. Meanwhile, the rate constant of H_2O oxidation in the anodic cell is 7.9738×10^{-11}. In addition, the study also found that the degradation cell undergoes polarization. It is indicated by the low value of the cathodic rate constant, i.e. 3.2805×10^{-10}. The cathodic cell is only filled with water, therefore, the reducing species is only H_2O molecules. The result also shows that Cu-TiO_2/Graphite also has adsorption ability in which the dye molecules were adsorbed with adsorption constant of 5.56×10^{-2} ppm^{-1}.

Keywords: reaction kinetics; photo-degradation; electro-degradation; photo-electro-degradation

Introduction

Many researches on photo-electrocatalytic degradation have been carried out, most are applied a regular reaction kinetics for chemical reaction with a pseudo first-order (Mohite et al., 2015; Lin et al., 2015) or a Langmuir-Hinshelwood equation (Quinones et al., 2010; Wang et al., 2014). Langmuir-Hinshelwood kinetics is the most commonly used expresion to explain the kinetics of heterogeneous catalytic system (Kumar et al., 2008), in which the reaction rate is a function of reactant concentration, as it is described in Eq. (1).

$$r = -\frac{dC}{dt} = \frac{krKC}{1+KC} \tag{1}$$

The k_r is the limiting rate constant of reaction at maximum coverage under the given experimental conditions. Meanwhile, *K* is the equilibrium constant for adsorption of the substrate onto catalyst (Kumar et al., 2008). This kinetics expression does not consider the effect of electric current as one of driving force for dye degradation. Meanwhile, in the photo-electro-assited degradation, there always a possibility of degradation due to electric driven, or the combination of electric and photo driven. In the study of kinetics of electrode reaction which is defined by Buttler-Volmer equation, the factor of current density is placed as important as the concentration factor, and it is described in the Buttler-Volmer equation (Eq. (2)) (Prentice, 1999).

$$r_{RR} = \frac{i_{RR}}{nF} = k_{RR} C_{RR}^{\ x} = k'_{RR} \exp\left\{\frac{(1-\beta)nF\Phi}{RT}\right\}[RR]^{x} \qquad (2)$$

K_{RR} is the rate constant of RR degradation, C_{RR} is concentration of RR 5B, i_{RR} is the current density recorded during reaction, r_{RR} is the rate of RR 5B reaction, *n* is the number of electrons involved in reaction, *F* is Faraday constant, Φ is the measured potential, β is the symmetry of electrochemical reaction and (1-β) refers to transfer coefficient of anodic components.

However, the possibility of organic molecules to be adsorbed onto catalyst surface before degradation can not be neglected, as the catalyst has ability for adsorption. In order to find the equilibrium constant of adsorption, *K,* and the rate constant, *k*, Langmuir isoterm of adsorption (Eq. (3)) (Hanoar et al., 2014) can be applied.

$$\theta = \frac{n_{ads}}{n_o} = \frac{K\,C_A}{1 + K\,C_A}; K = \frac{k_{ads}}{k_{des}} \qquad (3)$$

θ is the surface coverage, n_{ads} is the number of molecules adsorbed, n_o is the total number adsorption sites, C_A is concentration of adsorbate molecules, k_{ads} is the adsorption constant and k_{des} is the desorption constant. The rate of catalytic reaction is comparable to the surface coverage, therefore the rate law of the catalytic reaction is as defined by equation (3) which is named as Langmuir-Hinshelwood (L-H) equation (Eq. (4)) (Andrieux et al., 2011).

$$r = \frac{dC_{Ao}}{dt} = k\,\theta = \frac{k\,K\,C_A}{1 + K\,C_A} = k_{obs}\,C_A \qquad (4)$$

Integration of L-H equation is as in Eq. (5)

$$\ln\frac{C_{Ao}}{C_A} = k_{obs}t \qquad (5)$$

C_{Ao} is the initial concentration of adsorbate molecules, k is rate constant of adsorption, K is the equilibrium constant of adsorption and k_{obs} is rate constant of pseudo- first order of adsorption reaction (Mohite et al., 2015).

Due to the complexicity of photo-electro-degradation system, in this research authors have tried to apply the Buttler-Volmer equation for photo-electro-degradation of Remazol Red 5B. The electric current factor is represented by the measured potential, Φ. In this research the possibility of water oxidation or water reduction were also considered through detection pf proton production or hydroxide ions production. The different rate of anodic and cathodic reaction is known to cause cell polarization and furthermore decrease the efficiency of electrochemical cell [9], therefore in this research, the anodic reaction rate and cathodic reaction rate were studied to understand the possibility of cell polarization. Photocatalyst, TiO_2 layer that was modified by depositing Cu metal on it, was used as the photocatalyst material. In order to promote the electric current, therefore the photocatalyst layer was coated on graphite substrate. Graphite is a conductive and inert material, which means that it does not undergo electrochemical reaction during current application. Despite of boron doped diamond (Canizares et al., 2004), lead dioxide (Dai et al., 2012), and composite of exfoliated graphite-diamond (Ntsendwana et al., 2013), the carbon based materials such as activated carbon (Li et al., 2008), single wall carbon nano tube (Xiang et al., 2009), and also exfoliated graphite (Ntsendwana et al., 2016).

Experiment

The TiO_2/Graphite was prepared through chemical bath deposition as it was described in our previous paper (Rahmawatiet al., 2010). Titanium (IV) chloride (pro analysis grade, Merck) was used as titania precursor. The surfactant cetyl trimethylammonium bromide (CTAB, pro analysis grade, Merck) was added to the precursor solution in order to promote deposition of titania network on a graphite substrate. The titania network deposition was conducted in 60 ^oC for 4 days. The prepared TiO_2/Graphite then being characterized by XRD (Shimadzu XRD-6000) to ensure that TiO_2 film has been formed during the reaction, by comparing their diffraction patterns to diffraction standard of rutile and anatase TiO_2.

Cu was deposited on TiO_2 surface by electrodeposition of 0.4 M $CuSO_4$ solution. The applied current was 0.03 A. The TiO_2/Graphite was used as a cathode and a graphite rod was used as the anode. The electrodeposition was carried out in Electrolytic Analyser (Yanaco AES-2D) for 30 minutes. The prepared Cu-TiO_2/Graphite then was dried at room temperature. XRD analysis was conducted to ensure the presence of Cu, by comparing the XRD pattern with standard XRD pattern of Cu.

The λ_{max} absorption of RR 5B has been determined at 400 – 700 nm and it was founded at 512 nm. The degradation of RR 5B at various concentration, i.e 10, 15, 20 and 25 ppm has been carried out in isolation box. The Cu-TiO$_2$/Graphite tablet that used as an anode was dipped into 20 mL RR 5B solution. Meanwhile, in cathodic compartment, a graphite rod cathode was dipped in 20 mL of 0.1 M KCl solution. A 6 watt UV lamp 254 nm (9815 series) was used as light source. It was positioned 12 cm in front of the anodic cell. Both anodic and cathodic cell were connected by KCl solution salt bridge. The degradation was carried out for 140 minutes. In every 10 minutes, 5 mL of anodic solution was taken to be analyzed with UV Vis spectrophotometer (SP 300-Optima) at 512 nm. Also, in every 10 minutes the pH of anodic and cathodic solution was recorded with a digital pH meter (pH 207 Luxtron). The pH change in the anodic cell might represent oxidation of H_2O molecules. Meanwhile, the pH change in the cathodic cell might represent the reaction that occured during the degradation process.

Kinetics study on this Remazol Red 5B degradation was conducted by considering the possibility of electrodegradation reaction and also photodegradation reaction. Due to a high applied potential used, i.e 12 volt, therefore the reduction-oxidation of H_2O might occured to competes for the RR5B reaction. The Buttler-Volmer equation for kinetics, Eq. (1), was applied to measured the reaction rate of RR5B oxidation. In Buttler-Volmer equation, the symmetrical factor, β, to be assumed as 0.5 for cathodic and 0.5 for anodic. The possibility of H_2O electrooxidation might produce the symmetrical factor as in Eq. (6).

$$\begin{aligned} \beta_{A1} + \beta_{A2} &= 0.5 \\ \beta_{A1} = \beta_{A2} &= 0.25 \end{aligned} \tag{6}$$

where β_{A1} is the symmetrical factor of the oxidation of RR 5B and β_{A2} refers as oxidation of H_2O.

Therefore the reaction rate of RR 5B degradation as it is described in Eq. (2) can be defined further by Eq. (7).

$$r_{RR} = k'_{RR} \exp\left\{\frac{F\Phi}{4RT}\right\}[RR]^x \tag{7}$$

Meanwhile the rate constant, K_{RR}, is defined by Eq. (8).

$$k_{RR} = k'_{RR} \exp\left\{\frac{F\Phi}{4RT}\right\} \tag{8}$$

Therefore, the rate of RR 5B reaction follows Eq. (9).

$$r_{RR} = k_R\,[RR]^x \tag{9}$$

The RR concentration can be recorded as absorbance, A. For first order reaction, the integration method produces Eq. (10).

$$\mathrm{Ln}\,A = \ln A_o - k.t \tag{10}$$

A is absorbance, A_o is the initial absorbance of 20 ppm RR 5B solution, k is the rate constant and t is degradation time (minutes). Meanwhile, the integration method for second order produce Eq. (11). Determination of reaction order is based on its linear regression constant, R.

$$\frac{1}{A} = \frac{1}{A_o} + k\,t \tag{11}$$

If RR 5B degradation occured due to photon radiation and by the existence of hydroxy radical, OH•, as it is proposed by Wang et al. (2014), therefore, reactions (12) – (16) might be proposed.

$$\mathrm{TiO_2} + hv \rightarrow hole^+ + e^- \tag{12}$$

$$h^+ + \mathrm{H_2O} \rightarrow \mathrm{OH^\bullet} + \mathrm{H^+} \tag{13}$$

$$\mathrm{H_2O} \leftrightarrows \mathrm{H^+} + \mathrm{OH^-} \tag{14}$$

$$h^+ + \mathrm{OH^-} \rightarrow \mathrm{OH^\bullet} \tag{15}$$

$$\mathrm{OH^\bullet} + \mathrm{RR} \rightarrow \mathrm{RR^*}\ \text{(the degraded RR)} \tag{16}$$

Formation of OH• (Eq. (13)) can be identified by the change of pH of solution and Eq. (17) might be proposed.

$$\frac{d[\mathrm{OH}\bullet]}{dt} = k\,[\mathrm{H^+}]^x[\mathrm{OH}\bullet]^y \tag{17}$$

OH• is a very reactive molecule and they will proceed to the next reaction fastly, therefore Eq. (13) can be assume as zero order for OH• (Eq. (18)) and reaction can be followed from pH of solution.

$$\frac{d[\mathrm{OH}\bullet]}{dt} = k\,[\mathrm{H^+}]^x \tag{18}$$

Meanwhile, dissosiasion of water (Eq. (14)) has a very small possibility, due to a small dissosiation constant of water, i.e $K_w = 10^{-14}$. Therefore, Eq. (14) can be ignored. Rate law of Eq. (16) is described by Eq. (19).

$$-\frac{d[RR]}{dt} = k\,[\mathrm{OH}\bullet]^y[RR]^x \tag{19}$$

However, the reaction with radical proceed very fast and it is not the determining reaction. Meanwhile, if the excited electron in the conduction band contribute to the RR degradation, reaction (20)- (24) might be proposed.

$$e^{-} + O_2 \rightarrow O_2^{\bullet -} \tag{20}$$

$$2\,O_2^{\bullet -} + 2H_2O \rightarrow H_2O_2 + 2OH^{-} + O_2 \tag{21}$$

$$H_2O_2 + e^{-} \rightarrow OH^{-} + OH^{\bullet} \tag{22}$$

$$OH^{-} + h^{+} \longrightarrow \rightarrow OH^{\bullet} \tag{23}$$

$$OH^{\bullet} + RR \longrightarrow RR^{*} \text{ (the degraded RR)} \tag{24}$$

Reaction (20) produces radical oxygen which is unstable and will move fastly to the next reaction, Eq. (21) also proceed fastly. Hydrogen peroxide, H_2O_2, is a very reactive molecule and therefore react with electron fastly forming hydroxide ion and radical hydroxide (Eq. (22)). Therefore those (20), (21) and (22) are not the determining step of reaction. The formation of radical hydroxide in Eq. (22) might be followed from pH of solution as it is defined in Eq. (25).

$$\frac{d[OH\bullet]}{dt} = k\,[OH^{-}]^{z} \tag{25}$$

→ → → → →

Meanwhile the electrooxidation of H_2O might follow Buttler-Volmer reaction, as it is defined in Eq. (26).

$$r_{H2O} = \frac{i_{H2O}}{nF} = k_{H2O}[H_2O]^{y} = k'_{H2O} \exp\left\{\frac{(1-\beta)nF\Phi}{RT}\right\}[H_2O]^{y} \tag{26}$$

Since the contribution of H_2O oxidation to a symmetrical factor of electrochemical reaction, β, is 0.25, therefore Eq. (26) becomes Eq. (27).

$$r_{H2O} = k'_{H2O} \exp\left\{\frac{F\Phi}{2RT}\right\}[H_2O]^{y} \tag{27}$$

Rate law of H_2O oxidation is defined by Eq. (28)

$$r_{H2O} = k_{H2O}[H_2O]^{y} \tag{28}$$

where the k_{H2O} is rate constant and it is defined by Eq. (29)

$$k_{H2O} = k'_{H2O} \exp\left\{\frac{F\Phi}{2RT}\right\} \tag{29}$$

Based on H_2O oxidation reaction as it is described in Eq.(13), therefore the H_2O concentration can be detected from the pH change of anodic solution, as one mol of H_2O produces two moles of H^+ from dissociation reaction and from oxidation reaction by hole, h^+. The integral method to determined the reaction order is defined in Eq. (30) for the first order and in Eq. (31) for the second order.

$$\ln[H_2O] = \ln[H_2O]_o - k.t \tag{30}$$

$$\frac{1}{[H_2O]} = \frac{1}{[H_2O]_o} + k.t \tag{31}$$

Reduction of H_2O in cathodic electrochemically might follow Buttler-Volmer equation, as in Eq. (32).

$$r_c = k'_c \exp\left\{\frac{\beta nF\Phi}{RT}\right\}[H_2O]_o^{\,z} \tag{32}$$

$[H_2O]_o$ is the reducted H_2O molecules. With assumes that the symmetrical cathodic factor is 0.5, therefore Eq. (32) becomes Eq. (33).

$$r_c = k'_c \exp\left\{\frac{F\Phi}{2RT}\right\}[H_2O]_o^{\,z} \tag{33}$$

The cathodic reaction rate constant is defined by Eq. (34) and rate law of cathodic reduction of H_2O is defined by Eq. (35).

$$k_c = k'_c \exp\left\{\frac{F\Phi}{2RT}\right\} \tag{34}$$

$$r_c = k_c[H_2O]_o^{\,z} \tag{35}$$

The concentration of H_2O might be followed by pH change of cathodic solution which is converted to hydroxide ion concentration $[OH^-]$. The linear plot of an integral method for first and second order reaction are applied to determined the order of reaction.

Result and discussion

XRD diffraction pattern of Cu-TiO_2/Graphite and its morphology are described in Fig. 1. Peaks of Cu are identified at 2θ of 43.2^o. Gravimetrical analysis found that the mean weight of TiO_2 film is 3 ± 0.8 mg and mean weight of deposited Cu is 2 ± 0.5 mg.

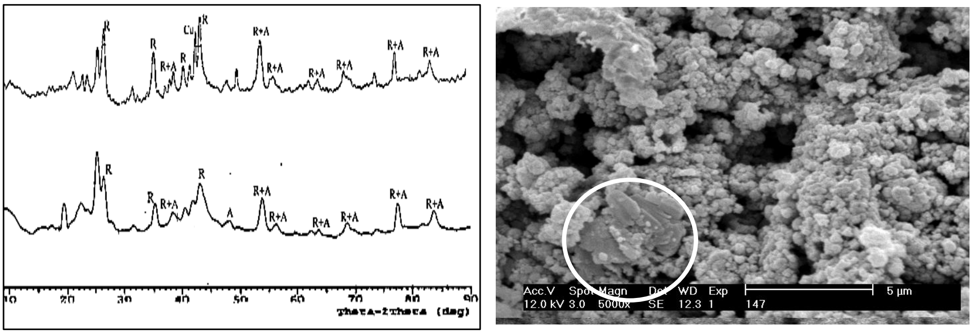

(a) (b)

Figure 1. XRD pattern of Cu-TiO$_2$/Graphite and TiO$_2$/Graphite, R is rutile, A is anatase, and Cu is the peak of deposited Cu (a) and the SEM image of its surface morphology, the white circle showing a deposite of Cu (b)

The absorbance of RR 5B solution decreased during photoelectrodegradation (Fig. 2). The pH of the anodic solution which was the RR 5B solution was decreased indicating that the oxidation of RR 5B molecules might release some protons, H$^+$ (Fig. 3(a)). Meanwhile, the pH of the cathodic solution was slighly increased, until around 7.2 (Fig. 3(b)). It is still in the category of a neutral solution, actually.

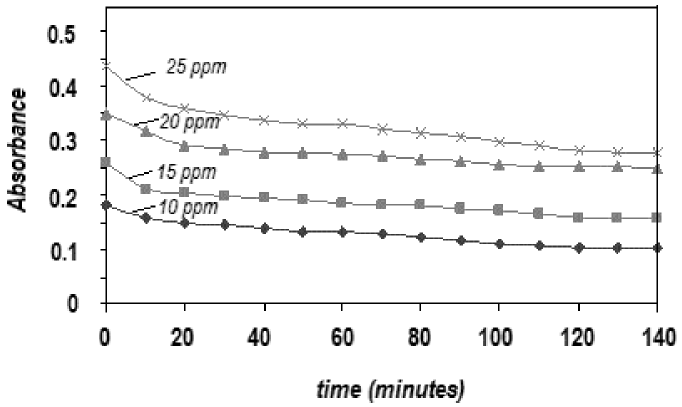

Figure 2. The absorbance data of RR 5B solution during photoelectrodegradation

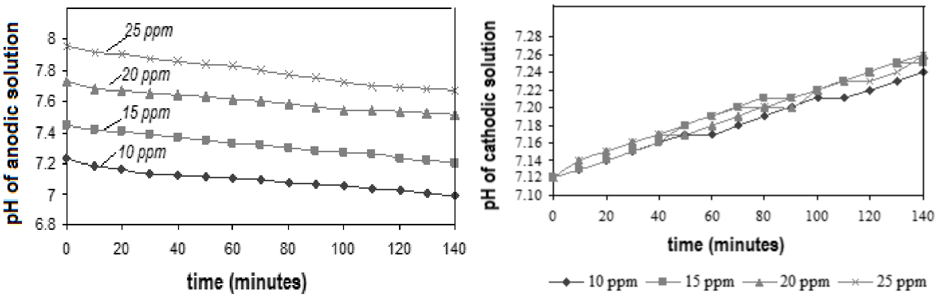

Figure 3. pH of RR5B solution (in anodic cell) (a) and pH of cathodic solution (b) during photoelectrodegradation

Mechanism of reduction-oxidation that can be proposed are the hole at valence band (h^{+}_{vb}) reacted with adsorbed water at the catalyst surface to form hydroxil radical ($OH^{\bullet}$). Meanwhile, the electrons in the conduction band (e^{-}_{cb}) reduced oxygen to form anionic superoxide radicals that could proceed to the hydroxil radicals formation trough some mechanism as described earler (Mohite et al., 2015). The redox reactions in degradation cell occured based on the redox potential of the hole (h^{+}_{vb}) and electron (e^{-}_{cb}). The reduction potential of the hole in TiO_2 in solution at pH of 7 is +2.53 V (vs standard hydrogen electrode, SHE) and the reduction potential of the electron (e^{-}_{cb}) is -0.52 V (vs SHE). It indicates that hole at the TiO_2 surface is a strong oxidator and will oxidize other species with smaller reduction potential including water an/or hydroxil group to produce the hydroxil radical. The hydroxy radical has a reduction potential of +2.27 V (vs SHE) and has the ability to oxidize some organic molecules.

The mechanism of photo-excitation in TiO_2 are described in Eqs. (36-40)) (Mohite et al., 2015).

$$TiO_2 + h\nu \rightarrow hole^{+} + e^{-} \tag{36}$$

$$h^{+} + H_2O \rightarrow OH^{\cdot} + H^{+} \tag{37}$$

$$H_2O \leftrightarrows H^{+} + OH^{-} \tag{38}$$

$$h^{+} + OH^{-} \rightarrow OH^{\cdot} \tag{39}$$

$$OH^{\cdot} + RR \rightarrow \text{smaller molecules} \tag{40}$$

The equilibrium constant of water dissosiation is very small i.e. 1.01×10^{-14}, therefore the possibility of reaction (37) to occurs was small. Due to the RR 5B solution was in anodic cell, therefore the RR 5B would be electrochemically oxidized and the proposed reactions are in Eqs. (41-45).

$$RR \rightarrow RR^{+} + e^{-} \tag{41}$$

$$2H_2O + 2e^{-} \rightarrow 2OH^{-} + H_2 \tag{42}$$

$$hole^{+} + OH^{-} \rightarrow OH^{\bullet} \tag{43}$$

$$OH^{\bullet} + RR \rightarrow \text{smaller molecules} \tag{44}$$

$$OH^{\bullet} + RR^{+} \rightarrow \text{smaller molecules} \tag{45}$$

Due to the degradation cell was open to the air, therefore it was possible if O_2 existed in the solution. If the excited electrons (e^{-}_{cb}) that reacted with oxygen (O_2) then the reaction occured would be as listed in Eqs. (46-52).

$$e^{-} + O_2 \rightarrow O_2^{\bullet -} \tag{46}$$

$$O_2^{\bullet -} + H^{+} \rightarrow HO_2^{\bullet} \tag{47}$$

$$2\,HO_2^{\bullet} \rightarrow H_2O_2 + O_2 \tag{48}$$

$$H_2O_2 + e^{-} \rightarrow OH^{-} + OH^{\bullet} \tag{49}$$

$$OH^{-} + h^{+} \rightarrow OH^{\bullet} \tag{50}$$

$$OH^{\bullet} + RR \rightarrow \text{smaller molecules} \tag{51}$$

$$OH^{\bullet} + RR^{+} \rightarrow \text{smaller molecules} \tag{52}$$

The mechanism proposed to formulate the rate law are as listed in Eqs. (53-56).

Mechanism 1:

$$OH^{\bullet} + RR \rightarrow \text{simple molecules} \tag{53}$$

Mechanism 2:

$$RR \rightarrow RR^{+} + e^{-} \tag{54}$$

$$OH^{\bullet} + RR^{+} \rightarrow \text{simple molecules} \tag{55}$$

Mechanism 1 produces rate law as written in Eq. (56).

$$r_{RR} = k_{RR\,.}\,[RR]^{x}.\,[OH^{\bullet}]^{y} \tag{56}$$

Molecules with the radical site have a very short life time, therefore the order to them can be defined as pseudo zero order. Therefore the rate law is pseudo x order to RR 5B, as written in Eq. (56).

$$r_{RR} = k_{RR\,.}\,[RR]^{x} \tag{57}$$

From mechanism 2, the reaction to RR is defined in equation (57) and (58).

$$\mathrm{RR} \rightarrow \mathrm{RR}^{+} + \mathrm{e}\,(\mathrm{slow}) \tag{58}$$

$$\mathrm{OH}^{\bullet} + \mathrm{RR}^{+} \rightarrow \text{ smaller molecules (fast)} \tag{59}$$

Reaction with radical molecules is usually proceed fast, then the determining step is the oxidation of RR 5B. Therefore the rate law is as written in Eq. (60).

$$r_{RR} = k_{RR\,.}\,[\mathrm{RR}]^{x} \tag{60}$$

Integration method found that for the first order and second order, the rate law follows Eqs. (61) and (62), respectively.

$$\mathrm{Ln\,A} = \mathrm{LnAo\text{-}kt} \tag{61}$$

$$1/\mathrm{A}{=}{-}1/\mathrm{Ao} + \mathrm{kt} \tag{62}$$

Plots of Eqs. (60) and (61) with linear regression application produced linearity constant, R, that can be used as parameter to defined the suitable reaction order.

In the anodic cell, H_2O was oxidized into H^+ and O_2 and released electrons (Eq. (63)). This reaction will change the pH of the anodic solution. It is in agreement with pH decreasing in the anodic cell as shown in Fig. 3(a).

$$2\mathrm{H_2O} \rightarrow 4\mathrm{H}^{+} + \mathrm{O_2} + 4\mathrm{e}^{-} \tag{63}$$

The rate constant of H_2O oxidation, k_{H2O}, was determined to calculate reaction order on each RR concentration. First order was determined by plotting $\ln[H_2O]$ as a function of time, and the second order was determined by plotting $1/[H_2O]$ as a function of time,t. It is known that, H_2O concentration was an abundance or too high in comparison to the concentration of RR 5B. Therefore, it concludes that the reaction is zero order to H_2O and the rate law is defined as written in Eqs. (63) and (64).

$$r_{H2O} = k_{H2O} \times \left[H_2O\right]_{oks}^{\;O} \tag{64}$$

$$r_{H2O} = k_{H2Ooks} \tag{65}$$

If reaction rate is defined as the function of H^+ production, therefore reaction rate can be written as Eqs. (66-68).

$$r_{H2O} = \tfrac{1}{2}\frac{d\left[H^{+}\right]}{dt} = k_{H2O} \tag{66}$$

$$\tfrac{1}{2} d\left[H^{+}\right] = k_{H2O} \times dt \tag{67}$$

$$\left[H^{+}\right] = 2.k_{H2O}\,.\mathrm{t} + \mathrm{c} \tag{68}$$

Linear regression of plot between $[H^+]$ versus time,t, resulted in slope value of $2.k_{H2O}$. The average value of k_{H2O} at each RR 5B concentration is the rate constant of oxidation rate of H_2O, $k_{H2O,\ oxidation}$.

In cathode cell, the H_2O reduced into OH^- and H_2, as depicted in Eq. (69).

$$2H_2O + 2e^- \rightarrow 2OH^- + H_2 \tag{69}$$

The rate constant of H_2O reduction, $k_{H2O,\ the\ reduction}$ was determined by the reaction order values found from integral method application at every RR 5B concentration. The first order calculation was conducted by plotting $\ln[H_2O]$ versus t (time). Meanwhile, the second order calculation was conducted by plotting $1/[H_2O]$ versus t (time). The rate constant found from the plot is almost constant at 3.2805×10^{-10}. Therefore, it is concluded that the H_2O follows zero order, as depicted in Eqs. (70-71).

$$r_{H2O} = k_{H2O} \times \left[H_2O\right]_{red}^{O} \tag{70}$$

$$r_{H2O} = k_{H2Ored} \tag{71}$$

The reaction rate of H_2O reduction (r_{H2O}) is linear to its rate constant. If the reaction rate is in the form of OH^- production, therefore it can be written as Eqs. (72-74).

$$r_{H2O} = \frac{d\left[OH^{-}\right]}{dt} = k_{H2O} \tag{72}$$

$$d\left[OH^{-}\right] = k_{H2O} \times dt \tag{73}$$

$$\left[OH^{-}\right] = k_{H2O}\,.\mathrm{t} + \mathrm{c} \tag{74}$$

The linear regression of $[OH^-]$ versus t would produce a slope to calculate the rate constant, k_{H2O}.

Kinetics of RR 5B degradation was determined by calculate comparison between anodic and cathodic rate (*ka/kc*) and determined the comparison of anodic rate and cathodic rate, *ra/rc*. The experiment detects that there are two reactions proceed in an anodic cell which is oxidation of RR 5B and oxidation of H_2O. Therefore, the reaction between them also being compared to know the dominant reaction occured. Rate constant values and their comparison are listed in Table 2. The rate constant of RR oxidation is larger than rate constant of H_2O oxidation. It indicates that RR oxidation was dominantly occured in the anodic cell. The similar phenomena also occured in the cathodic cell, in which the reduction of RR 5B proceeds much faster than the reduction of H_2O.

Table 2. Rate constant of each reaction predicted in anodic and cathodic cell

$k_{H2O_{OKS}}$	k_{RR}	$k_{H2O_{RED}}$	$\frac{k_{RR}}{k_{H2O\,oks}}$	$\frac{k_{RR}}{k_{H2O\,red}}$	$\frac{k_{H2Ooks}}{k_{H2O\,red}}$
7.9738×10^{-11}	2.7795×10^{-3}	3.2805×10^{-10}	3.4858×10^{7}	8.4728×10^{6}	0.2431

Meanwhile, by applying Butler-Volmer equation, the reaction rate of oxidation and reduction can be calculated and listed in Table 3.

Table 3. Rate of reaction in anodic and cathodic cell

[RR] (ppm)	$r_{H2O_{OKS}}$	r_{RR}	$r_{H2O_{RED}}$	$\frac{k_{RR}}{k_{H2O\,oks}}$	$\frac{k_{RR}}{k_{H2O\,red}}$	$\frac{r_{H2O_{OKS}}}{r_{H2O\,red}}$
10	7.9738×10^{-11}	2.7795×10^{-2}	3.2805×10^{-10}	3.4858×10^{8}	8.4728×10^{7}	0.2431
15	7.9738×10^{-11}	4.1693×10^{-2}	3.2805×10^{-10}	5.2287×10^{8}	1.2709×10^{7}	0.2431
20	7.9738×10^{-11}	5.5590×10^{-2}	3.2805×10^{-10}	6.9716×10^{8}	1.6946×10^{7}	0.2431
25	7.9738×10^{-11}	6.9488×10^{-2}	3.2805×10^{-10}	8.7145×10^{8}	2.1182×10^{8}	0.2431

Table 3 shows that oxidation and reduction rate of H_2O are constant, because those are zero order to H_2O concentration. Meanwhile, the oxidation and reduction of RR 5B are a function of RR 5B concentration. In order to investigate polarization phenomena that frequently occur in the electrochemical system, therefore the anodic reaction rate, r_{OKS}, was compared to cathodic reaction rate, r_{red}. The result is listed in Table 3. The value is 0.2431. It indicates that RR 5B oxidation proceed faster than RR 5B reduction, or the electrochemical system was polarized. Polarization that occurs due to the difference of anodic and cathodic reaction rate is namely as kinetic polarization.This can be reduced by stirring the solution during electrochemical process.

The effect of RR 5B concentration to the reaction rate can be seen from Table 4. Photocatalytic oxidation of organic molecules by TiO_2 has been investigated by some researchers and it was found that the relation between initial concentration and rate law can be explained by Langmuir-Hinshelwood Kinetics (Topalov et al., 2000). Table 4 shows that the oxidation rate of RR 5B increases with the increasing of initial concentration of RR 5B. It indicates that when the dye concentration increased, there are many dye molecules undergo excitation and transfer of energy.

Table 4. Rate of reaction as function of RR 5B concentration

[RR] (ppm)	r ×10^2 (ppm menit-1)
10	2.7795
15	4.1693
20	5.5590
25	6.9488

The mechanism that possibly occured, the molecules were adsorbed by the catalyst before they were degraded. Langmuir Isoterm of adsorption can be used to determined the equilibrium constant of adsorption, K, and the rate constant of adsorption, *k'*.

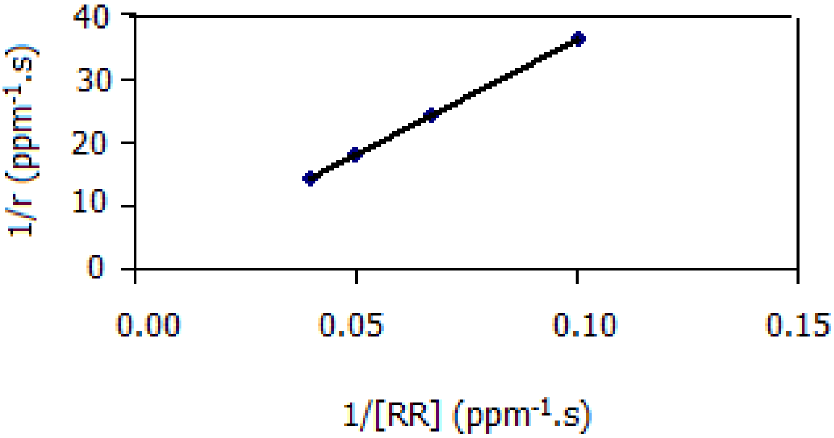

Figure 5. Langmuir isoterm of adsorption

The values of *k'* and K were determined from the intercept of the linear plot between 1/r and 1/[RR] as described in in Figure 5. The values of *k'* and K are 0.05 ppm.min^{-1} and 5.56 ×10^{-2} ppm^{-1} (mol.dm^{-3}), respectively. The rate constant that was found from observation or named as the k_{obs} is 2.80 ×10^{-3} min^{-1} . The k_{obs} are the K times *k'* which was determined by the plot in Figure 5. The Langmuir-Hinshelwood kinetics shows that the RR 5B molecules were adsorbed on the Cu-TiO_2/graphite surface before degradation. It is supported by adsorption data of RR 5B on Cu-TiO_2/graphite. The adsorption was conducted without providing light radiation and applied current. The adsorption plot is depicted in Figure 6. The adsorption curve shows that the absorbance, A, of RR5B decreased until the minutes of 30, and then it becomes constant.

The K value in this research is smaller than the values of Methylene Blue adsorption on TiO_2 powder, i.e. 1.79×10^4 dm^3 mol^{-1} for K and 3.36×10^{-8} mol dm^3 s^{-1} for *k'* (Lakshmi et al., 1995). Meanwhile, Topalov et al. (2000) found the K and *k'* values of 0.315 dm^3 $mmol^{-1}$ dan 1.80×10^{-2} mmol dm^{-3} min^{-1}, respectively, for adsorption of herbicide mecoprop on TiO_2 nanopowder. The small L-H constant kinetics on this research shows that TiO_2 in layer form has lower adsorption capacity than in the powder form.

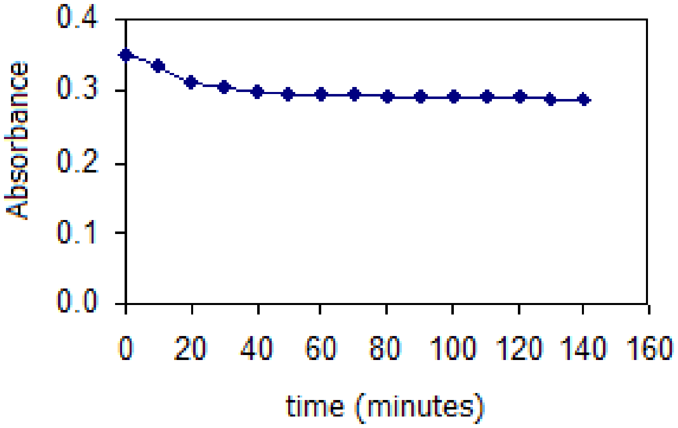

Figure 6. Adsoprtion of RR 5B molecules on Cu-TiO_2 surface

Conclusion

During photoelectrodegradation, the H_2O molecules were oxidized in competition with the dye oxidation. However, the dye oxidation proceeds faster than H_2O oxidation. The rate constant of dye oxidation is 2.7795×10^{-3}. Meanwhile, the rate constant of H_2O oxidation in the anodic cell is 7.9738×10^{-11}. This kinetics study also found that the degradation cell was polarized, in which the cathodic rate constant, i.e. 3.2805×10^{-10}, is lower than the oxidation rate in anodic cell. The ability of Cu-TiO_2/Graphite to absorp dye molecules is low with absorption constant only 5.56×10^{-2} ppm^{-1} ($mol.dm^{-3}$). Layer form of the catalyst might become the reason for the low absorption ability.

REFERENCES

Andrieux, J., Demirci, U.B. & Miele, P. (2011). Langmuir-Hinshelwood kinetic model to capture the cobalt nanoparticle-catalyzed hydrolysis of sodium borohydride over a wide temperature range. *Cat. Today, 170,* 13 – 19.

Cañizares, P., Sáez, C., Lobato, J. & Rodrigo, M.A. (2004). Electrochemical treatment of 4-nitrophenol aqueous wastes using boron-doped diamond anodes. *Ind. & Eng. Chem. Res, 43,* 1944 – 1951.

Dai, Q., Xia, Y., Jiang, L., Li, W., Wang, J. & Chen, J. (2012). Enhanced degradation of aspirin by electrochemical oxidation with modified PbO_2 electrode and hydrogen peroxide. *Int. J. Electrochem. Sci, 7,* 12895 – 12906.

Hanaor, D.A.H., Ghadiri, M., Chrzanowski, W. & Gan, Y. (2014). Scalable surface area characterization by electrokinetic analysis of complex anion adsorption. *Langmuir, 30,* 15143 – 15152.

Kumar, K.V., Porkodi, K. & Rocha, F. (2008). Langmuir-Hinshelwood kinetics - a theoretical study. *Cat. Comm., 9,* 82 – 84.

Li, L-t., Hao, L-n., Zhang, J., Wang, G.c. & Xie, Q. (2008). Preparation and electrochemical properties of the activated carbon doped with manganese. *New Carbon Materials, 23,* 269 – 274.

Lin, C.J., Liao, S.-J., Kao, .L.-C. & Liou, S.Y.H. (2015). Photoelectrocatalytic activity of a hydrothermally grown branched ZnO nanorod-array electrode for paracetamol degradation. *J. Hazardous. Mat, 291,* 9 – 17.

Mohite, V.S., Mahadik, M.A., Kumbhar, S.S., Hunge, Y.M., Kim, J.H., Moholkar, A.V., Rajpure, K.Y. & Bhosale, C.H.(2015). Photoelectrocatalytic degradation of benzoic acid using Au doped TiO_2 thin films. *J. Photochem. Photobiol. B, 142,* 204 – 211.

Ntsendwana, B., Mamba, B.B., Sampath, S. & Arotiba, O.A. (2013). Synthesis, characterisation and application of an exfoliated graphite–diamond composite electrode in the electrochemical degradation of trichloroethylene. *RSC Adv, 3,* 24473 – 24483.

Ntsendwana, B., Peleyeju, M.G. & Arotiba, O.A. (2016). The application of exfoliated graphite electrode in the electrochemical degradation of *p*-nitrophenol in water. *J. Environ. Sci. Health. Part A, 51,* 571 – 578.

Prentice, G.A. (1990). *Electrochemical engineering principles*. Upper Saddle River: Prentice Hall.

Quinones, C., Ayala, J. & Vallejo, W. (2010). Methylene blue photoelectrodegradation under UV irradiation on Au/Pd-modified TiO_2 films. *Appl. Surf. Sci., 257,* 367 – 371.

Rahmawati, F., Kusumaningsih, T., Hapsari, A.M. & Hastuti, A. (2010). Ag and Cu loaded on TiO2/graphite as a catalyst for Escherichia coli-contaminated water disinfection. *Chem. Papers, 64,* 557 – 565.

Stern, M. & Geary, A.L. (1957). Electrochemical polarization I: a theoretical analysis of the shape of polarization curves. *J. Electrochem. Soc., 104*, 56 – 63.

Topalov, A., Molnár-Gábor, D., Kosanić, M. & Abramović, B. (2000). Photomineralization of the herbicide mecoprop dissolved in water sensitized by TiO_2. *Water Res., 34,* 1473 – 1478.

Wang, X., Li, G., Zhu, H., Yu, J.C., Xiao, X. & Li, Q. (2014). Vertically aligned CdTe nanotube arrays on indium tin oxide for visible-light-driven photoelectrocatalysis. *Appl. Cat. B,, 147,* 17 – 21.

Xiang, D.-y., Su, Z., Zhao, Z., Yang, L.-q. &Yang, Q-h. (2009). Preparation of a SWCNT-DNA modified electrode and its electrochemical detection property. *New Carbon Materials, 24,* 183 – 186.

✉ **Dr. Fitria Rahmawati (corresponding author)**
Research Group of Solid State Chemistry & Catalysis
Chemistry Department
Sebelas Maret University
36 A, Jl. Ir. Sutami Kentingan
57126 Surakarta, Indonesia
E-mail: fitria@mipa.uns.ac.id